(2)

OFFICE OF NAVAL RESEARCH

Grant N00014-90-J-1193

TECHNICAL REPORT No. 27

Theoretical Studies of Electron Transport in Quantum-Well Structures

by

Lakshmi N. Pandey, Mark I. Stockman, Thomas F. George and Devaraj Sahu

Prepared for Publication

in

Proceedings of the Xth Vavilov Conference on Nonlinear Optics
Edited by S. G. Rautian
Novosibirsk, West Siberia, USSR

Departments of Chemistry and Physics
State University of New York at Buffalo
Buffalo, New York 14260

October 1990

UNCLASSIFIED
SECURITY CLASSIFICATION OF THIS PAGE

REPORT DOCUMENTATION PAGE

Form Approved OMB No. 0704-0188

1a. REPORT SECURITY CLASSIFICATION: Unclassified	1b. RESTRICTIVE MARKINGS
2a. SECURITY CLASSIFICATION AUTHORITY	3. DISTRIBUTION/AVAILABILITY OF REPORT: Approved for public release; distribution unlimited
2b. DECLASSIFICATION/DOWNGRADING SCHEDULE	
4. PERFORMING ORGANIZATION REPORT NUMBER(S): UBUFFALO/DC/90/TR-27	5. MONITORING ORGANIZATION REPORT NUMBER(S)
6a. NAME OF PERFORMING ORGANIZATION: Depts. Chemistry & Physics, State University of New York; 6b. OFFICE SYMBOL (If applicable)	7a. NAME OF MONITORING ORGANIZATION
6c. ADDRESS (City, State, and ZIP Code): Fronczak Hall, Amherst Campus, Buffalo, New York 14260	7b. ADDRESS (City, State, and ZIP Code): Chemistry Program, 800 N. Quincy Street, Arlington, Virginia 22217
8a. NAME OF FUNDING/SPONSORING ORGANIZATION: Office of Naval Research; 8b. OFFICE SYMBOL (If applicable)	9. PROCUREMENT INSTRUMENT IDENTIFICATION NUMBER: Grant N00014-90-J-1193
8c. ADDRESS (City, State, and ZIP Code): Chemistry Program, 800 N. Quincy Street, Arlington, Virginia 22217	10. SOURCE OF FUNDING NUMBERS: PROGRAM ELEMENT NO. / PROJECT NO. / TASK NO / WORK UNIT ACCESSION NO.

11. TITLE (Include Security Classification)

Theoretical Studies of Electron Transport in Quantum-Well Structures

12. PERSONAL AUTHOR(S)

Lakshmi N. Pandey, Mark I. Stockman, Thomas F. George and Devaraj Sahu

13a. TYPE OF REPORT	13b. TIME COVERED	14. DATE OF REPORT (Year, Month, Day)	15. PAGE COUNT
	FROM _____ TO _____	October 1990	7

16. SUPPLEMENTARY NOTATION: Prepared for publication in *Proceedings of the Xth Vavilov Conference on Nonlinear Optics*, Edited by S. G. Rautian, Novosibirsk, West Siberia, USSR

17. COSATI CODES		
FIELD	GROUP	SUB-GROUP

18. SUBJECT TERMS (Continue on reverse if necessary and identify by block number)

QUANTUM-WELL STRUCTURES; DWELL TIME; ELECTRON TRANSPORT; FAST FOURIER TRANSFORM METHOD; TUNNELING; TIME-DEPENDENT STUDY

19. ABSTRACT (Continue on reverse if necessary and identify by block number)

The study of resonant tunneling structures (RTS) has become increasingly important because of possible device applications and also because of the basic physics they involve. Within the static picture we have calculated the dwell time, i.e., the average time an electron spends inside an RTS. The actual time involved in the tunneling process can be described by the solution of the time-dependent effective mass Schrödinger equation (TDEMSE), and a code based on the fast Fourier transform method is developed to solve the TDEMSE for a potential profile such as RTS. The physical properties of an RTS investigated are the build-up time, which is the time taken by an electron to accumulate probability inside the well, and the escape time.

20. DISTRIBUTION/AVAILABILITY OF ABSTRACT	21. ABSTRACT SECURITY CLASSIFICATION
☒ UNCLASSIFIED/UNLIMITED ☒ SAME AS RPT. ☐ DTIC USERS	Unclassified
22a. NAME OF RESPONSIBLE INDIVIDUAL: Dr. David L. Nelson	22b. TELEPHONE (Include Area Code): (202) 696-4410; 22c. OFFICE SYMBOL

DD Form 1473, JUN 86 — Previous editions are obsolete. — SECURITY CLASSIFICATION OF THIS PAGE

UNCLASSIFIED

Theoretical Studies of Electron Transport in Quantum-Well Structures

Lakshmi N. Pandey,* Mark I. Stockman,*‡ Thomas F. George*† and Devaraj Sahu**
* Departments of Physics & Astronomy and Chemistry
Center for Electronic and Electro-optic Materials
State University of New York at Buffalo, Buffalo, New York 14260, USA
** Computer Sciences Corporation, 10110 Aerospace Road
Lanham-Seabrook, Maryland 20706,USA

The study of resonant tunneling structures (RTS) has become increasingly important because of possible device applications and also because of the basic physics they involve. Within the static picture we have calculated the dwell time, i.e., the average time an electron spends inside an RTS. The actual time involved in the tunneling process can be described by the solution of the time-dependent effective mass Schödinger equation (TDEMSE), and a code based on the fast Fourier transform method is developed to solve the TDEMSE for a potential profile such as RTS. The physical properties of an RTS investigated are the build-up time, which is the time taken by an electron to accumulate probability inside the well, and the escape time.

1. Introduction

How long it takes for a moving particle to penetrate a potential barrier is a question being asked often since the discovery of alpha particles. Recently, interest in investigating the time scale involved in the tunneling process was revived after the work of Tsu and Esaki,[1] where they explained the negative differential resistance in the $I-V$ characteristic of a compound semiconductor diode through the resonant tunneling process. Since then, several statical and dynamical physical properties of resonant tunneling structures (a single well formed by two barriers of finite widths and heights,[2] henceforth referred to as RTS) have been the subject of investigation. A vast literature[3,4] is available by now on the field. Our main interest here is to answer the question above, although the time scale involved in the resonant tunneling process is the most controversial topic still today. We have studied through a static picture the most accepted dynamical quantity, the dwell-time, which is the average time spent by an electron inside an RTS. A dynamical aspect of the problem is also addressed by the solution of the one-dimensional time dependent effective mass Schrodinger equation (TDEMSE), and the properties investigated from the solution are the build-up time, which is the time taken by an electron to accumulate probability inside the well, and the escape time, which is on a time scale associated with the resonance width through the uncertainty principle.

2. Static Picture and Dwell-Time

As mentioned above, the dwell time is an average time during which the probability to find the electron inside an RTS is finite. Hence, the dwell time is the total probability of the electron per unit incident flux.[5] The stationary-state properties of an RTS in the effective mass approximation are obtained by solving the time-independent Schrodinger equation for the envelop function $\Psi(x)$ along the growth direction x :[6,7]

$$-\frac{1}{\hbar^2}m^a\frac{d}{dx}m^b\frac{d}{dx}m^a\Psi(x)+[V(x)-E]\Psi(x)=0\ , \qquad (1)$$

where $V(x)$ is the RTS potential profile

$$V(x) = \begin{cases} V_1, & \text{if } 0 \le x \le a_1 \ , \\ 0, & \text{if } a_1 \le x \le a_1 + d \ , \\ V_2, & \text{if } a_1 + d \le x \le a_1 + d + a_2 \ , \end{cases}$$

V_i and a_i (i=1,2) are the heights and widths of the barriers, d is the width of the well, m is effective mass, and $2a + b = -1$ with a and b as constants. These constants must appear in the form given in order to keep the Hamiltonian Hermitian. The kinetic energy operator of Eq. (1) dictates that $m^a \Psi(x)$ and $m^{a+b} \frac{d\Psi(x)}{dx}$ must be continuous across the interface, implying the physical result that the current density $j \propto \frac{\Psi^*}{m} \frac{d\Psi}{dx} = m^a \Psi^* m^{a+b} \frac{d\Psi}{dx}$ be continuous. However, in general, the charge density $\rho \propto \Psi^* \Psi$ need not be continuous across an interface. For the special case of $a = 0$ and $b = -1$ one obtains, in addition, the continuity of charge density. So, this is a single-parameter b ($a = -\frac{1+b}{2}$) problem. The resonance states clearly depend on this parameter b, and one can not, *a priori*, prefer one value of b over another.

We have studied the dependence of the dwell time and width of the resonance on b. The dwell time τ_D over the region of 0 to x_1 of the structure is defined[4] as the integrated probability density of the electron per unit incidence flux,

$$\tau_D = \frac{m}{\hbar k} \int_0^{x_1} dx \ \mid \Psi(x) \mid^2 \ , \tag{2}$$

where $k = \sqrt{\frac{2mE}{\hbar^2}}$. Figures 1 and 2, and 3 and 4 show the dwell time as a function of x for three different b parameter values, -2, 0 & 2, and width of the resonance as a function of b for the first and second resonance states, respectively. It is clear from Figs. 1 and 3 that the dwell time varies considerably as one changes b, but a reverse pattern is found (Figs. 2 and 4) in the change of resonance widths of the first and second resonances.

We have thus shown that the parameter associated with the boundary conditions has a profound effect on the characteristics of the system such as resonance energy and width, and dwell time. It has been shown[8] in a different context that for two semi-infinite heterostructures, the boundary conditions at the interface not only involve the effective masses but also certain other parameters which are microscopic in origin, having no macroscopic analogs. We therefore believe that the arbitrariness in the choice of the parameter b can be fixed through microscopic calculations.

2. Dynamic Picture and Build-up and Escape Times

For b =0 and constant mass throughout the RTS, Eq. (1) with $E = i\hbar \frac{\partial}{\partial t}$ is solve numerically with the fast Fourier transform method.[9] When using this method, it has been found convenient to model a discontinuous potential, such as an RTS, as a combination of Fermi distribution functions of the form

$$\frac{V(x)}{V_0} = \frac{1}{\exp[(x - x_0 - c/2)/\delta] + 1} - \frac{1}{\exp[(x - x_0 + c/2)/\delta] + 1}$$

$$- \frac{1}{\exp[(x - x_0 - d/2)/\delta] + 1} + \frac{1}{\exp[(x - x_0 + d/2)/\delta] + 1} \ , \tag{3}$$

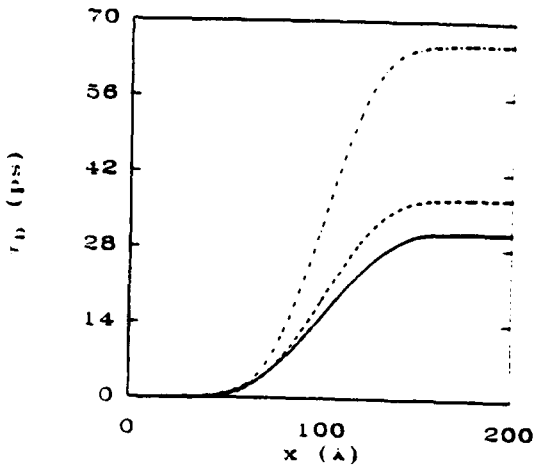

Fig. 1. Dwell-time as a function of position x for the first resonance state. The solid, dashed and dot-dashed lines are for b = -2, 0 and 2, respectively. The other parameters are: $a_1 = a_2$=50 Å, d= 100 Å.

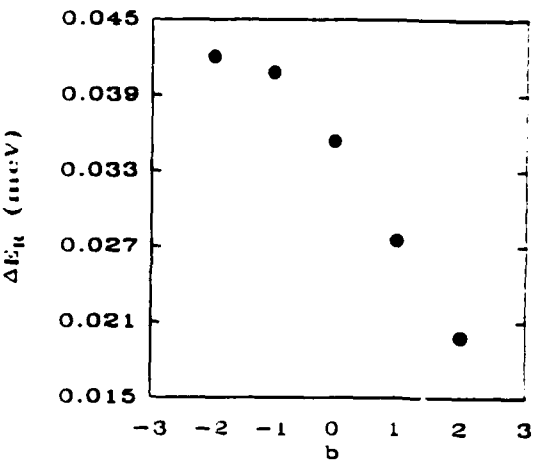

Fig. 2. Width of the first resonance state as a function of b.

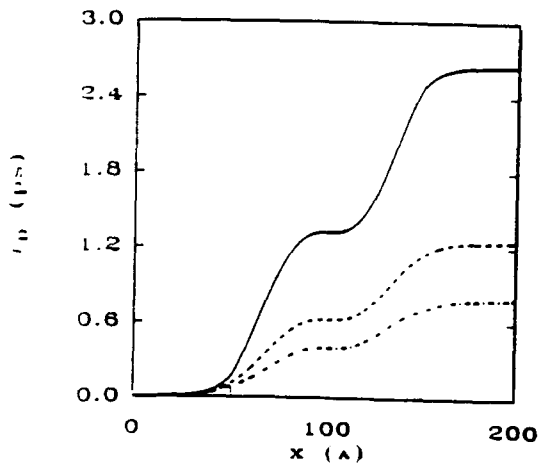

Fig. 3. Same as in Fig. 1 but for the second resonance state.

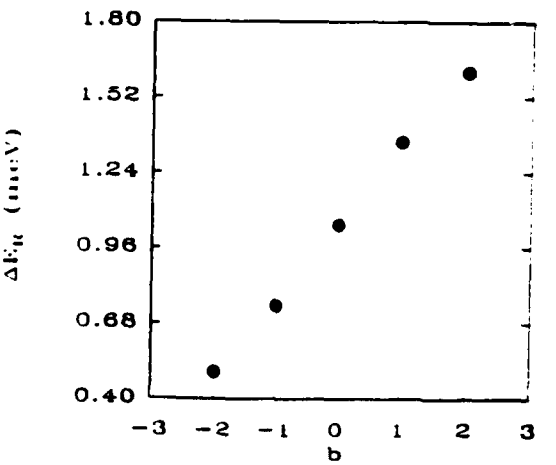

Fig. 4. Width of the second resonance state as a function of b.

where, $V_0 = V_1 = V_2$ is the barrier height, $c = a_1 + d + a_2$ is the total length of the RTS, x_0 is the position of the middle of the RTS, and δ is a smoothing parameter. We have carried out a single-step calculation using 1024 grid points, 20 out of which are used to discretize the RTS, with 10 out of this 20 to discretize the well in the RTS. Here δ is taken to be 2 Å, and a box of length 10240 Å corresponding to a grid spacing of 10 Å has been chosen for this calculation. These parameters are found appropriate to demonstrate the dynamics of an electron in a box which has a symmetric RTS located at its center.

To study the transport properties of an electron, we have chosen its initial wavefunction to be represented by a Gaussian wavepacket,

$$\Psi(x, t = 0) = N \exp[\frac{-(x - x_p)^2}{4\sigma^2} + ik_0 x] \quad , \tag{4}$$

where x_p is the center of the wavepacket (one fourth of the box length from the left wall), σ is the width of the wavepacket, k_0 is the mean wave vector ($\Delta k = \frac{1}{\sigma}$), and N is a normalization factor. The wavefunction $\Psi(x, t)$ has been calculated for different values of t.

A symmetric RTS with $c = 200$ Å, $d = 100$ Å and $V_0 = 200$ meV is analyzed. There are two resonance states at 30.87 ± 0.174 meV and 117.4 ± 2.98 meV of the RTS considered here. Figures 5 and 6 display the integrated probability density $P(t) = \int_{x_0 - d/2}^{x_0 + d/2} dx |\Psi(x, t)|^2$ inside the well, which is part of the wavefunction trapped in the well as a function of time for the first and second resonance states, respectively. The transmission probability $T(t) = \int_{x_0 + c/2}^{\infty} dx |\Psi(x, t)|^2$ is also shown in Figs. 5 and 6 by dotted lines. It is clear that $P(t)$ increases up to a certain value P_{max}, and the time taken to reach P_{max} from a reference point is called the buildup-time τ_b. The probability $P(t)$ decays exponentially after the build-up time, and an exponential fit to the decay part of $P(t)$ versus time, $P(t) = P_{max} \exp(-\theta t)$, yields θ=0.264 and 4.5 ps^{-1} and hence, the width of the state $\Delta E_R = 0.174$ and 2.98 meV for the first and second resonance states, respectively. Since the first resonance state is sharp in energy, it takes more time to decay, during which the reflected and transmitted parts of the wavepacket return back from the box wall. To avoid interferences with the returned reflected and transmitted parts of the wavepacket, instead of allowing $P(t)$ to decay further, a fitted curve is shown by the dot-dashed line in Fig. 5.

In Figure 7, we show (a) the maximum probability density P_{max} trapped in the well in the upper panel and (b) the transmission probability along with the plane wave transmission coefficient (solid line) in the lower panel as a function of the electron energy in the neighborhood of the second resonance state for $\sigma = 400$ (solid circles), 500 (open circles) and 600 (solid triangles) Å. The lower panel also displays the exact transmission coefficient T^σ for a wavepacket[10] with σ= 400 (dashed line), 500 (dotted line) and 600 (dot-dashed line) Å. The resonance energy of $T(t)$ in the lower panel of Fig. 7 is slightly shifted from the T^σ because of the reason that the Fermi distributed structure as in Eq. (3) is not a exact representation of the RTS used to calculate the plane wave transmission coefficient and T^σ. The transmission probability T(t) associated with the dynamics and exact transmission coefficient T^σ are expected to coalesce with the plane wave transmission coefficient in the limit of an infinitely-extended ($\sigma \rightarrow \infty$) wavepacket. The distribution P_{max} as a function of energy peaks at the resonance energy, and the width (FWHM) of this

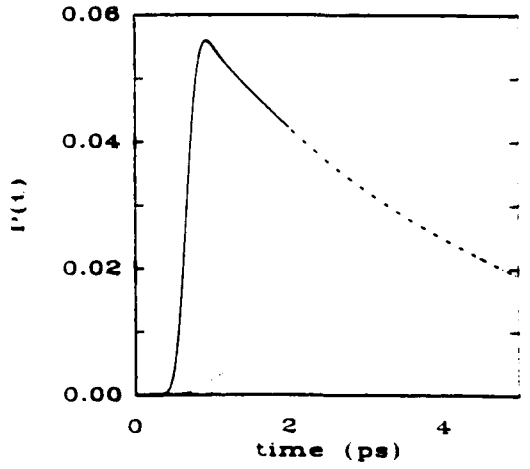

Fig. 5. Integrated probability $P(t)$ inside the well as a function of time. The mean energy and width of the incident packet are the energy of the first resonance state and 400 Å, respectively. The dot-dashed line is an extrapolation of $P(t)$.

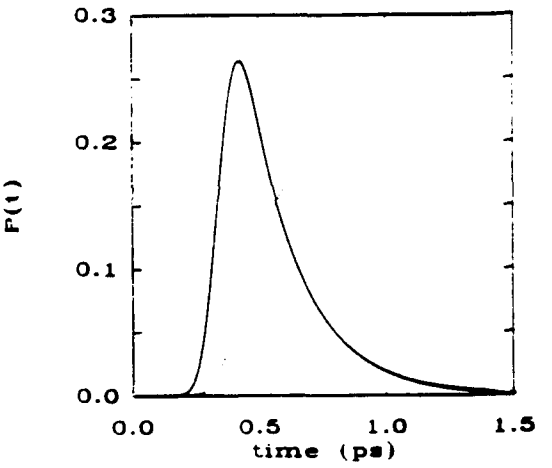

Fig. 6. Integrated probability $P(t)$ inside the well as a function of time. The mean energy and width of the incident packet are the energy of the second resonance state and 400 Å, respectively.

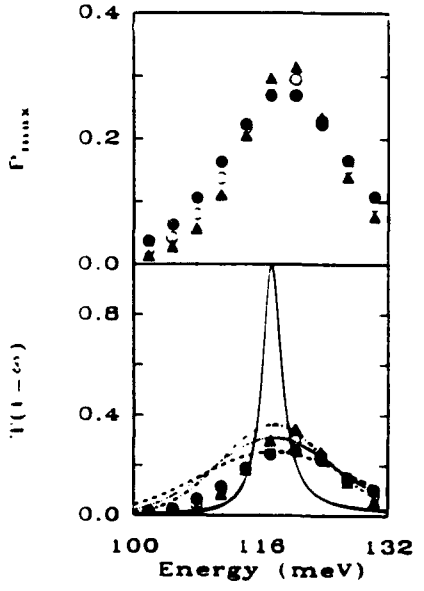

Fig. 7. P_{max} in the upper panel and $T(t=\infty)$ in the lower panel as a function of the mean energy. The solid line shows the plane wave transmission coefficients. The dashed, dotted and dot-dashed lines in the lower panel are T^{σ} for $\sigma = 400$, 500 and 600 Å, respectively. The solid circles, open circles and solid triangles represent the results of σ = 400, 500 and 600 Å, respectively.

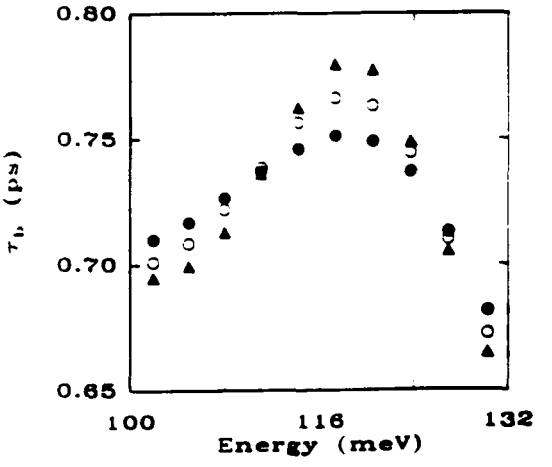

Fig. 8. Build-up time as a function of the mean energy. The explanation of the points is the same as in Fig. 7.

distribution decreases as σ increases. This is a consequence of resonant tunneling, because for the case of on-resonance scattering, a substantial portion of the wavepacket tunnels through the first barrier, whereas for off-resonance, most of the packet gets reflected by the first barrier.

The resonance tunneling process can further be demonstrated by looking at τ_b as a function of packet mean energy, as displayed in Fig. 8 for energies in the vicinity of the second resonance state and σ = 400, 500 and 600 Å. This τ_b also peaks at the resonance energy, which can not be explained through simple dynamics but must involve the resonance tunneling. In a simple dynamical picture, energetic the particle takes less time to to travel a path filled with obstacles (repulsive potential profile such as an RTS), whereas in the case of resonance tunneling, the electron with energy equal to the resonance energy bounces back and forth from the walls of the well, since its wavefunction is negligible at the walls in comparison with the rest of the places in the well, and it takes much more time to accumulate probability than the electrons with energies off-resonance.

In conclusion, we have shown here a dynamical picture of a resonance tunneling process. The probability inside the well decays exponentially, and excellent agreement is found between the decay constant and the static width of the resonance. We have also demonstrated that the transmission probability coalesces with the plane wave transmission coefficient in the limit of an infinitely-extended wavepacket.

Acknowledgments

This research was supported by the U.S. Office of Naval Research. The calculation for the solution of the TDEMSE was done utilizing the facilities at the Pittsburgh Supercomputing Center under Grant No. PHY890020P.

References

‡ Also with Institute of Automation & Electrometry, Siberian Branch of the USSR Academy of Sciences, 630090 Novosibirsk, USSR.

† Talk presented by Thomas F. George.

1. R. Tsu and L. Esaki, Appl. Phys. Lett. **22**, 562 (1973).
2. The barrier height depends on y, the fraction of *Al* in the layer of *AlGaAs* forming the barrier. The number of monolayers of *AlGaAs* and *GaAs* define the widths of the barrier and well, respectively. The formulae $V_i(eV) = 0.65(1.155y + 0.37y^2)$ and $m = 0.067 + 0.088y$ are used to calculate the barrier height and effective mass.
3. Gerald Bastard, *Wave Mechanics Applied to Semiconductor Heterostructures* (Les Editions de Physique, Les Ulis, France, 1988) and references therein.
4. E. H. Hauge and J. A. Støvneng, Rev. Mod. Phys. **61**, 917 (1989) and references therein.
5. L. N. Pandey, D. Sahu and T. F. George, Solid State Comm. **72**, 7 (1989).
6. R. A. Morrow and K. R. Brownstein, Phys. Rev. B **30**, 678 (1984).
7. G. Bastard, Phys. Rev. B **24**, 5693 (1981).
8. W. Trzeciakowski, Phys. Rev. B **38**, 4322 (1988); R. A. Ginberg and S. Luryi, Phys. Rev. B **39**, 7466 (1989).
9. F. Ancilotto, A. Selloni, L. F. Xu and E. Tosati, Phys. Rev. B **39**, 8322 (1989).
10. The exact transmission coefficient for a wavepacket of width σ can be calculated by $T^\sigma = \int_{-\infty}^{\infty} dk \mid \Psi_{k_0} \mid^2 T(k)$ where $\Psi_{k_0} = N \exp[-\sigma^2(k - k_0)^2]$ is the wavepacket in k-space and $T(k)$ is the plane wave transmission coefficient for the RTS.

TECHNICAL REPORT DISTRIBUTION LIST - GENERAL

Office of Naval Research (2)
Chemistry Division, Code 1113
800 North Quincy Street
Arlington, Virginia 22217-5000

Commanding Officer (1)
Naval Weapons Support Center
Dr. Bernard E. Douda
Crane, Indiana 47522-5050

Dr. Richard W. Drisko (1)
Naval Civil Engineering Laboratory
Code L52
Port Hueneme, CA 93043

David Taylor Research Center (1)
Dr. Eugene C. Fischer
Annapolis, MD 21402-5067

Dr. James S. Murday (1)
Chemistry Division, Code 6100
Naval Research Laboratory
Washington, D.C. 20375-5000

Dr. David L. Nelson (1)
Chemistry Division
Office of Naval Research
800 North Quincy Street
Arlington, Virginia 22217

Dr. Robert Green, Director (1)
Chemistry Division, Code 385
Naval Weapons Center
China Lake, CA 93555-6001

Chief of Naval Research (1)
Special Assistant for Marine Corps Matters
Code 00MC
800 North Quincy Street
Arlington, VA 22217-5000

Dr. Bernadette Eichinger (1)
Naval Ship Systems Engineering Station
Code 053
Philadelphia Naval Base
Philadelphia, PA 19112

Dr. Sachio Yamamoto (1)
Naval Ocean Systems Center
Code 52
San Diego, CA 92152-5000

Dr. Harold H. Singerman (1)
David Taylor Research Center
Code 283
Annapolis, MD 21402-5067

Defense Technical Information Center (2)
Building 5, Cameron Station
Alexandria, VA 22314

FY90 Abstracts Distribution List for Solid State & Surface Chemistry

Professor John Baldeschwieler
Department of Chemistry
California Inst. of Technology
Pasadena, CA 91125

Professor Paul Barbara
Department of Chemistry
University of Minnesota
Minneapolis, MN 55455-0431

Dr. Duncan Brown
Advanced Technology Materials
520-B Danury Rd.
New Milford, CT 06776

Professor Stanley Bruckenstein
Department of Chemistry
State University of New York
Buffalo, NY 14214

Professor Carolyn Cassady
Department of Chemistry
Miami University
Oxford, OH 45056

Professor R.P.H. Chang
Dept. Matls. Sci. & Engineering
Northwestern University
Evanston, IL 60208

Professor Frank DiSalvo
Department of Chemistry
Cornell University
Ithaca, NY 14853

Dr. James Duncan
Federal Systems Division
Eastman Kodak Company
Rochester, NY 14650-2156

Professor Arthur Ellis
Department of Chemistry
University of Wisconsin
Madison, WI 53706

Professor Mustafa El-Sayed
Department of Chemistry
University of California
Los Angeles, CA 90024

Professor John Eyler
Department of Chemistry
University of Florida
Gainesville, FL 32611

Professor James Garvey
Department of Chemistry
State University of New York
Buffalo, NY 14214

Professor Steven George
Department of Chemistry
Stanford University
Stanford, CA 94305

Professor Tom George
Dept. of Chemistry & Physics
State University of New York
Buffalo, NY 14260

Dr. Robert Hamers
IBM T.J. Watson Research Center
P.O. Box 218
Yorktown Heights, NY 10598

Professor Paul Hansma
Department of Physics
University of California
Santa Barbara, CA 93106

Professor Charles Harris
Department of Chemistry
University of California
Berkeley, CA 94720

Professor John Hemminger
Department of Chemistry
University of California
Irvine, CA 92717

Professor Roald Hoffmann
Department of Chemistry
Cornell University
Ithaca, NY 14853

Professor Leonard Interrante
Department of Chemistry
Rensselaer Polytechnic Institute
Troy, NY 12181

Professor Eugene Irene
Department of Chemistry
University of North Carolina
Chapel Hill, NC 27514

Dr. Sylvia Johnson
SRI International
333 Ravenswood Avenue
Menlo Park, CA 94025

Dr. Zakya Kafafi
Code 6551
Naval Research Laboratory
Washington, DC 20375-5000

Professor Larry Kesmodel
Department of Physics
Indiana University
Bloomington, IN 47403

Professor Max Lagally
Dept. Metal. & Min. Engineering
University of Wisconsin
Madison, WI 53706

Dr. Stephen Lieberman
Code 522
Naval Ocean Systems Center
San Diego, CA 92152

Professor M.C. Lin
Department of Chemistry
Emory University
Atlanta, GA 30322

Professor Fred McLafferty
Department of Chemistry
Cornell University
Ithaca, NY 14853-1301

Professor Horia Metiu
Department of Chemistry
University of California
Santa Barbara, CA 93106

Professor Larry Miller
Department of Chemistry
University of Minnesota
Minneapolis, MN 55455-0431

Professor George Morrison
Department of Chemistry
Cornell University
Ithaca, NY 14853

Professor Daniel Neumark
Department of Chemistry
University of California
Berkeley, CA 94720

Professor David Ramaker
Department of Chemistry
George Washington University
Washington, DC 20052

Dr. Gary Rubloff
IBM T.J. Watson Research Center
P.O. Box 218
Yorktown Heights, NY 10598

Professor Richard Smalley
Department of Chemistry
Rice University
P.O. Box 1892
Houston, TX 77251

Professor Gerald Stringfellow
Dept. of Matls. Sci. & Engineering
University of Utah
Salt Lake City, UT 84112

Professor Galen Stucky
Department of Chemistry
University of California
Santa Barbara, CA 93106

Professor H. Tachikawa
Department of Chemistry
Jackson State University
Jackson, MI 39217-0510

Professor William Unertl
Lab. for Surface Sci. & Technology
University of Maine
Orono, ME 04469

Dr. Terrell Vanderah
Code 3854
Naval Weapons Center
China Lake, CA 93555

Professor John Weaver
Dept. of Chem. & Mat. Sciences
University of Minnesota
Minneapolis, MN 55455

Professor Brad Weiner
Department of Chemistry
University of Puerto Rico
Rio Piedras, Puerto Rico 00931

Professor Robert Whetten
Department of Chemistry
University of California
Los Angeles, CA 90024

Professor R. Stanley Williams
Department of Chemistry
University of California
Los Angeles, CA 90024

Professor Nicholas Winograd
Department of Chemistry
Pennsylvania State University
University Park, PA 16802

Professor Aaron Wold
Department of Chemistry
Brown University
Providence, RI 02912

Professor Vicki Wysocki
Department of Chemistry
Virginia Commonwealth University
Richmond, VA 23284-2006

Professor John Yates
Department of Chemistry
University of Pittsburgh
Pittsburgh, PA 15260